Footprints of the QCD Crossover on Cosmological Gravitational Waves at Pulsar Timing Arrays

Gabriele Franciolini [1,*] Davide Racco [2,†] and Fabrizio Rompineve [3,4,5,‡]

[1]*Dipartimento di Fisica, Sapienza Università di Roma and INFN, Sezione di Roma, Piazzale Aldo Moro 5, 00185, Rome, Italy*
[2]*Stanford Institute for Theoretical Physics, Stanford University, 382 Via Pueblo Mall, Stanford, California 94305, USA*
[3]*CERN, Theoretical Physics Department, Esplanade des Particules 1, Geneva 1211, Switzerland*
[4]*Departament de Física, Universitat Autònoma de Barcelona, 08193 Bellaterra, Barcelona, Spain*
[5]*Institut de Física d'Altes Energies (IFAE) and The Barcelona Institute of Science and Technology (BIST),
Campus UAB, 08193 Bellaterra (Barcelona), Spain*

Pulsar timing arrays (PTAs) have reported evidence for a stochastic gravitational wave (GW) background at nanohertz frequencies, possibly originating in the early Universe. We show that the spectral shape of the low-frequency (causality) tail of GW signals sourced at temperatures around $T \gtrsim 1$ GeV is distinctively affected by confinement of strong interactions (QCD), due to the corresponding sharp decrease in the number of relativistic species, and significantly deviates from $\sim f^3$ commonly adopted in the literature. Bayesian analyses in the NANOGrav 15 years and the previous international PTA datasets reveal a significant improvement in the fit with respect to cubic power-law spectra, previously employed for the causality tail. While no conclusion on the nature of the signal can be drawn at the moment, our results show that the inclusion of standard model effects on cosmological GWs can have a decisive impact on model selection.

Introduction.—A stochastic background of gravitational waves (GWB) may be the only direct probe into the early stages of cosmological evolution, where it can be produced by physics beyond the standard model (SM). The recently reported evidence for a nanohertz GWB in the NANOGrav 15 years [1,2] (NG15), European PTA data release 2 (EPTA-DR2) [3,4], Parkes [5,6], and Chinese [7] PTA datasets, whose uncorrelated component was already detected with previous data [8–11], has attracted ample attention in the astrophysics, cosmology, and particle physics communities.

One of the most urgent endeavors is determining whether the signal is of cosmological or astrophysical origin, in the latter case sourced by supermassive black hole binaries (SMBHBs); see, e.g., [12,13] for an overview. This is difficult for multiple reasons. First, while the NG15 analysis suggests that the astrophysical model may face challenges [14], the current understanding of SMBHBs is not sufficiently precise to draw conclusions [11,15,16]; second, the spectrum of a cosmological GWB generically depends on the microphysical nature of the source and often requires case-by-case numerical simulations.

In this Letter, we show that a distinctive signature is nonetheless imprinted model independently by the early-Universe dynamics of the SM, in the GW spectra of a broad class of early-Universe sources. These are often referred to as causality limited, i.e., radiating GWs on timescales comparable to the corresponding Hubble time. Examples are first-order phase transitions (PTs) [17], annihilation of cosmic domain walls [18], collapse of large density perturbations [19] (see also [16,20–33]), and several well-motivated beyond the SM (BSM) scenarios (see instead [16,26,34–37] for PTA-related analyses of other types of possible cosmological GWBs).

Our starting point is a fortuitous coincidence of scales: The nanohertz frequencies probed by PTAs coincide with those of GWs that reenter the Hubble horizon at the epoch of the QCD crossover phase transition, i.e., at temperatures $T \sim 100$ MeV (see, e.g., [38]). While the crossover is not expected to source GWs, the rapid drop of relativistic degrees of freedom in the thermal bath significantly changes the equation of state (EOS) of the Universe, that is precisely determined by means of lattice QCD [39].

A causality-limited GW source, active before the QCD crossover, produces a model-independent low-frequency GW signal, which we refer to as the causality tail (CT), that is affected by the SM-induced change in the EOS. The CT spectrum is altered by the redshift of the SM radiation bath

(previously pointed out for other GW signals [40–42]) and the different evolution of GWs [43–45].

This Letter derives the spectral shape of CT signals at nanohertz frequencies, that can be readily used by PTA collaborations, GW, and BSM communities for model comparison (improving upon simple power-law CTs, currently adopted by NG15 [26] and EPTA-DR2 [16]; see also [21,22]). Importantly, we show that our novel inclusion of QCD-induced features significantly impacts the interpretation of current PTA data, by performing a Bayesian search for a CT signal in the international PTA data release 2 (IPTA-DR2) [11,46] and NG15 [2].

Standard model features in the causality tail of primordial GW backgrounds.—For cosmological GWBs, a powerful property is ensured in a broad class of primordial sources where GWs are generated locally, independently in each spatial patch, and in a limited amount of time. We denote by f_{CT} the frequency of GWs entering the Hubble radius when emission shuts off. The remarkable property of the CT is that GWs with frequencies $f < f_{CT}$ evolve independently of the source, because the corresponding wavelengths are larger than the source's correlation length. The evolution of each tensor mode $h_k(t)$ in this regime is sensitive only to the expansion of the Universe and GW propagation [41,47–76]. Cosmological PTs are a typical example [59,67,77,78]. In this case, bubble collisions, sound waves, and plasma turbulence act as causality-limited sources, each with its own finite correlation length.

The GW energy fraction is customarily defined as

$$\Omega_{GW}(f) \equiv \frac{1}{\rho_{cr}} \frac{d\rho_{GW}(f)}{d\ln f}, \qquad (1)$$

where ρ_{cr} is the critical energy density today. $\Omega_{GW}(f)$ exhibits a spectral shape, that is typically peaked at some frequency $f_\star > f_{CT}$. The CT of the spectrum behaves as $\Omega_{GW}(f \lesssim f_{CT}) \propto f^3$ in a universe filled by a perfect relativistic fluid with EOS $w(t) = p/\rho = \frac{1}{3}$; see, e.g., [51].

This tilt of the CT can be modified by two effects: (i) The GW energy density $\rho_{GW}(f)$ in the CT is determined by the Universe's expansion history and the GW propagation [43]; (ii) the critical energy density $\rho_{cr} = \rho_{\gamma,0}/\Omega_{\gamma,0}$ in Eq. (1) [where $\Omega_{\gamma,0}h^2 = 2.47 \times 10^{-5}$ is the SM radiation abundance today and $h \equiv H_0/(100 \text{ km/s/Mpc})$ is the reduced Hubble constant] is affected by entropy injections originating, e.g., from freeze-out processes occurring for (B)SM particles in the thermal bath [41].

The first effect concerns the evolution of super-Hubble tensor modes [43]. After the GW source shuts off, the emitted super-Hubble modes freeze due to Hubble friction, remain practically constant until horizon reentry, and then proceed with underdamped oscillations diluted as $1/a$. As a result, the CT scales as
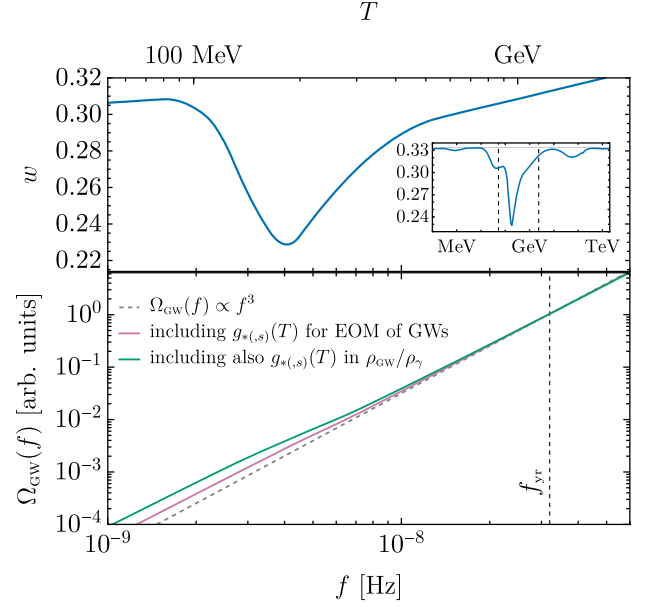

FIG. 1. Top: EOS during the QCD crossover. The inset shows w in an expanded range of temperatures. Bottom: impact of the variation of $w(T)$ and $g_\star(T)$ on the CT of a primordial GWB (plotted with an arbitrary amplitude). The dashed line shows the f^3 scaling obtained in a pure radiation-dominated universe.

$$\frac{d\rho_{GW}(f)}{d\ln f}\bigg|_{f<f_{CT}} \propto f^{3+2[(3w-1)/(3w+1)]} \qquad (2)$$

for a generic w. This scaling is additionally affected by relativistic free-streaming particles, as discussed below.

The second effect concerns only the SM radiation bath, since GWs are decoupled. This leads to a temperature-dependent modulation

$$\Omega_\gamma(T) = \Omega_{\gamma,0} \left(\frac{g_{\ast,s}(T_0)}{g_{\ast,s}(T)}\right)^{4/3} \left(\frac{g_\ast(T)}{g_\ast(T_0)}\right) \left(\frac{a_0}{a}\right)^4, \qquad (3)$$

$g_\ast(T) = \rho/(\pi^2 T^4/30)$ and $g_{\ast,s}(T) = s/(2\pi^2 T^3/45)$ being the effective number of degrees of freedom in energy (ρ) and entropy (s) densities, respectively, and $a(a_0)$ is the scale factor (today). From the thermodynamical relation $sT = p + \rho$, one infers the temperature-dependent EOS $w(T) = \frac{4}{3}[g_{\ast,s}(T)/g_\ast(T)] - 1$.

During the QCD crossover, heavy hadrons form and both $g_{\ast,s}(T)$ and $g_\ast(T)$ decrease rapidly. Their values, and the EOS shown in Fig. 1, are precisely determined with lattice QCD techniques [39]. The temporary decrease of $w(T)$ is due to the pressureless contribution of QCD matter to the thermal bath, followed by its rapid depletion. Therefore, the CT is distinctively modified, when the corresponding GWs with wave number k reenter the Hubble horizon during the QCD crossover. Their frequency is set by $f = k/2\pi = aH/2\pi$, which in terms of temperatures reads (see [79])

$$f \simeq 3.0 \text{ nHz} \cdot \left(\frac{g_{*,s}(T)}{20}\right)^{1/6} \left(\frac{T}{150 \text{ MeV}}\right). \quad (4)$$

We solve the equations of motion for $h_k(t)$ (see [79]), accounting for the temperature dependence of w and g_*, and obtain the spectrum shown in Fig. 1. A clear deviation from the commonly employed f^3 approximation is found, accidentally located in the nanohertz range where PTA experiments are most sensitive.

Beside the SM effects presented above, a nanohertz CT signal probes the cosmic expansion history back to $\sim T_{\text{QCD}}$. In particular, the possible presence of a fraction $f_{\text{FS}} \equiv \rho_{\text{FS}}/\rho_{\text{tot}}$ of free-streaming species [43] (including the irreducible contribution from GWs at frequencies higher than the CT ones) is easily accounted for, as explained in [79]. We tabulate the CT spectrum, shown in Fig. 1, in [79].

GWBs at PTAs.—PTA collaborations typically assume a power-law GW strain (see [79] for the relevant definitions) that implies a GWB

$$\Omega_{\text{CGW}}(f)h^2 \simeq 6.3 \times 10^{-10} \left(\frac{A_{\text{CGW}}}{10^{-15}}\right)^2 \left(\frac{f}{f_{\text{yr}}}\right)^{n_T}, \quad (5)$$

where $f_{\text{yr}} \equiv (1 \text{ yr})^{-1} \simeq 32$ nHz. For a cosmological GWB, we use the subscript CGW rather than CP. While a GWB from SMBHBs is expected, its properties are not yet fully known. In particular, population synthesis studies predict a wide range for amplitude and tilt [11,12,15,16,26,123–127]. The simple prediction $n_T = \frac{2}{3}$ is valid only for a continuous population with circular orbits and GW-driven energy loss [128].

The causality tail (CT) of a CGW is commonly modeled as a power law with $n_T = 3$. The main novelty of our work is that the actual CT is significantly different, when f_{CT} lies above the frequency bins employed in PTA analyses, i.e., 10 nHz $\lesssim f_{\text{CT}} \lesssim f_\star$, and this can impact the data fit relative to the simple $n_T = 3$ approximation that had been used previously.

A crucial difference between astrophysical and CGW backgrounds is that *only* the latter contribute to the energy budget in the early Universe and can affect cosmological observables as any other relativistic free-streaming component beyond the SM. CGWs contribute to the *effective number of neutrino species* as $N_{\text{eff}} \equiv 3.044 + \Delta N_{\text{eff}}^{\text{CGW}}$, with $\Delta N_{\text{eff}}^{\text{CGW}} = \rho_{\text{CGW}}/\rho_{\nu,1}$ and $\rho_{\nu,1}$ is the energy density of a single neutrino species. Specifically, the total (integrated) GW abundance is $\Omega_{\text{CGW}} h^2 \simeq 1.6 \times 10^{-6}(\Delta N_{\text{eff}}^{\text{CGW}}/0.28)$ [59]. Measurements of the cosmic microwave background (CMB) [129] and baryon acoustic oscillations (BAO) constrain $\Delta N_{\text{eff}} \leq 0.28$ at 95% C.L. For the peaked sources of interest, $\Omega_{\text{CGW}} \simeq \Omega_{\text{CGW}}(f_\star)$ and the constraint on CGW backgrounds reads
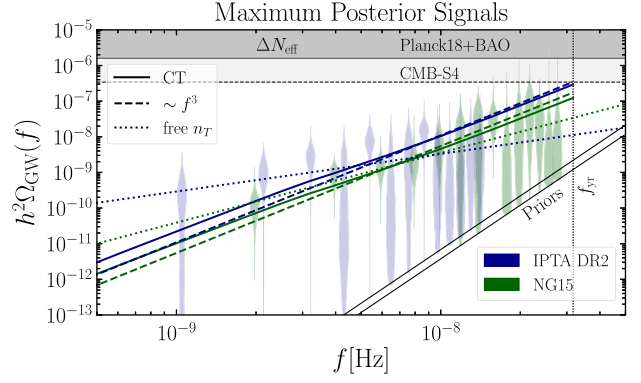

FIG. 2. The GW spectrum for the CT (solid line), $n_T = 3$ (dashed line), and free power-law (dotted line) models, selecting the maximum posterior values obtained with IPTA-DR2 [11] (blue) and NG15 [2] (green) datasets. The shaded region shows the CMB + BAO bound on ΔN_{eff}, and the dotted line the reach of CMB-S4 experiments. The lower limits of the posteriors are determined by the priors of [2,11]. See Fig. 3 for parameter posteriors.

$$A_{\text{CGW}} \leq 5 \times 10^{-14} \left(\frac{f_{\text{yr}}}{f_\star}\right)^{n_T/2} \quad (95\% \text{ C.L.}), \quad (6)$$

for signals that can be approximated with power laws up to $f_\star$. While this assumption is often not valid (see, e.g., [130,131] for PTs), the $\Delta N_{\text{eff}}^{\text{CGW}}$ bound can be applied model independently to the CT, thereby giving $A_{\text{CT}} \leq 5 \times 10^{-14}(f_{\text{yr}}/f_{\text{CT}})$. This often captures the approximate strength of the constraint, since typically $f_{\text{CT}} \lesssim (0.1-1)f_\star$ and the spectrum flattens close to the peak. By comparison with Eq. (5), it is evident that CMB constraints can affect signal interpretation when $f_{\text{CT}} \gtrsim f_{\text{yr}}$, if $n_T > 0$ (see also [132]).

Bayesian analysis.—We now discuss the relevance of our results when performing Bayesian analyses of IPTA-DR2 [11] and the recent NG15 [2] datasets. We do not consider other datasets such as EPTA-DR2 [4] and PPTA [6] which are broadly compatible, although less stringent, than NG15 [133]. We aim to quantify the impact of the QCD-induced deviations from a power law with $n_T = 3$ on signal interpretation, following the procedure of the PTA collaborations.

We compare the CT model to the power law $n_T = 3$, both with only one free parameter, A_{CT} and A_{CGW}, respectively. We impose ΔN_{eff} constraints in (below) Eq. (6) to A_{CGW} (A_{CT}). We set $f_{\text{CT}} = f_{\text{yr}}$ (such that the first bins of both datasets are deep in the CT) and similarly $f_\star = f_{\text{yr}}$ for the $n_T = 3$ model and comment on other choices below. We also compare CT with common power-law processes with free exponent n_T, as well as with $n_T = \frac{2}{3}$. For the NG15 analysis only, we also contrast CT with the SMBHB expectation obtained by the NG15 Collaboration [26], via population synthesis studies assuming circular orbits

and GW-only energy loss. Reference [79] lists all parameters and prior choices.

The GW spectra for maximum-posterior values of parameters obtained by our analyses are shown in Fig. 2. Both plots show why the CT presented in our work is expected to improve the fit to PTA data, when compared to the $n_T = 3$ power law: For $A_{\mathrm{CT}} = A_{\mathrm{CGW}}$, the CT allows for a larger amplitude of Ω_{GW} in the first bins (roughly by a factor of 2–3).

In Fig. 3, we show the posterior distribution for the relevant signal parameters of the models considered. For a qualitative comparison, one can approximate the CT as a power law with slope evaluated through a given number of frequency bins. The result of this procedure is shown by the vertical gray lines in Fig. 3, obtained by fitting the CT with a power law through the lowest fourth to eighth frequency bins of NG15, where evidence for GWs is reported. The 1, 2, and 3σ posteriors on power-law parameters reported by IPTA-DR2 and NG15 are also shown. We expect the CT to provide as good a fit to the NG15 data as a power-law model with parameters inside the 2σ region of the posteriors, whereas the f^3 signal lies at the border of the 3σ region. We stress that this is only approximate, since the CT deviates significantly from a power law at the relevant frequencies.

We finally compare models by computing the Bayes factors $\mathcal{B}_{ij}$, quantifying the preference of model i with respect to model j. These are reported in Table I. One important result is the comparison between the CT and power-law $n_T = 3$ signals. As highlighted in bold in Table I, the CT provides, in a statistically significant way, a better fit than f^3 to both datasets.

Testing against the possible astrophysical interpretation of the GWB is subject to uncertainties on the SMBHB signal. For NG15, no substantial evidence in favor of nor against the CT is observed in comparing with the SMBHB expectation of [26] and the $n_T = \frac{2}{3}$ model, while the evidence for a free power law over the CT is substantial. On the other hand, both power-law models are favored over the CT in the older IPTA-DR2. Most importantly, the result for $n_T = 3$ is strongly disfavored with respect to a generic power-law fit, while it becomes only mildly disfavored when the proper CT is considered. This shows that the inclusion of the unavoidable QCD effects is appreciable and can both qualitatively and quantitatively change the comparison between CGW from localized sources and the data. Future data releases will have more constraining power to further test the compatibility of the CT signal with the observations.

Let us comment on how different f_{CT} values affect our model comparison. The CMB bound on power-law CGW s becomes stronger for $f_{\mathrm{CT}} > f_{\mathrm{yr}}$, as shown in Fig. 3 for peak frequency $f_\star = 1, 3 f_{\mathrm{yr}}$. For the NG15 dataset, the CT signal is excluded at 3σ only if $f_{\mathrm{CT}} \gtrsim 100$ nHz. The future reach of CMB-S4 [134] observations is also plotted. One
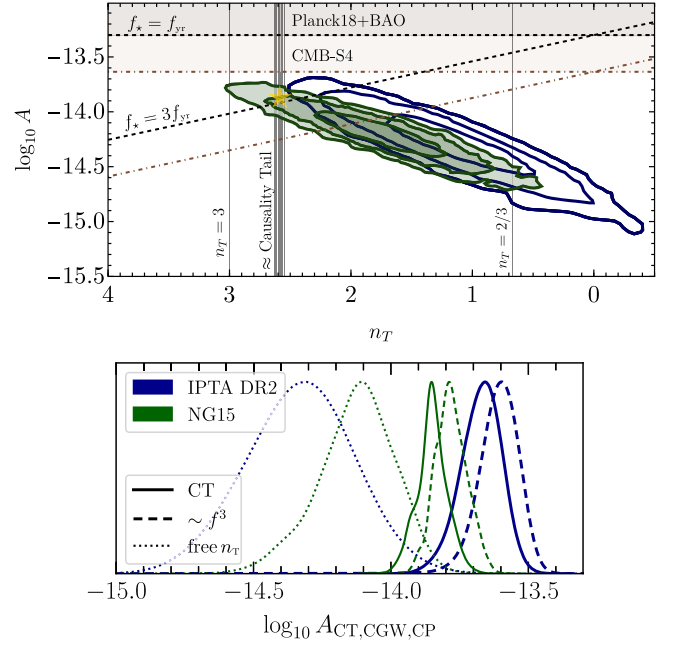

FIG. 3. Upper: 2D posterior for a power-law model for IPTA-DR2 [11] and NG15, the latter enforcing Hellings-Downs (HD) correlations in the analysis [2,4]. The vertical lines indicate approximations of the CT. The yellow star shows the best-fitting CT amplitude. We show current (dashed line) and future (dot-dashed line) ΔN_{eff} bounds affecting any power-law signal extending up to $f_\star = 1, 3 f_{\mathrm{yr}}$. The excluded region lies above the corresponding line. Lower: 1D posteriors on A for the power-law model (marginalizing over the second parameter n_T) and for the CT and f^3 models. The smaller amplitude observed for the free n_T case follows from the $A - n_T$ degeneracy observed in the upper panel, and the arbitrary choice of defining the spectral amplitude at f_{yr}; see Eq. (5).

could instead consider $f_\star < f_{\mathrm{yr}}$, in which case the peak of the signal would lie within the range of frequencies constrained by NG15. However, such analysis would be model dependent, as the properties of the GWB peak are controlled by the specific source under consideration. We leave such investigation for future work.

We note that the best-fit models, corresponding to the curves in Fig. 2, are associated to negligible values of f_{FS} from GWs of frequency $f = f_{\mathrm{CT}}$. Additional contributions from high-frequency and other free-streaming species are model dependent but would affect our results only if $\Delta N_{\mathrm{eff}}^{\mathrm{CGW}} \gtrsim 0.1$. In this case, an excess in upcoming cosmological surveys [134–136] is expected.

Discussion and implication for particle physics.—We have pointed out that SM physics predicts a specific shape for the CT of a GW signal, clearly distinguishable from $\Omega_{\mathrm{GW}} \sim f^3$ already with present datasets. This applies to any GW source that is active before QCD confinement (i.e., $T \gtrsim$ GeV; see [79]) and provides a much-needed signature to help determining whether the current PTA excess is of cosmological or astrophysical origin. If the SMBHB

TABLE I. $\log_{10}(\mathcal{B}_{\text{causality tail},\mathcal{M}})$ for the comparison of the CT with alternative models. The CT spectrum (see Fig. 1) is clearly distinguishable (*strong* Bayesian preference) from $\Omega_{\text{GW}} \sim f^3$.

	$\mathcal{M}$			
PTA	$n_T = 3$ ($\gamma = 2$)	Free n_T	$n_T = \frac{2}{3}$ [$\gamma = (13/3)$]	SMBHB (GW-driven)
IPTA-DR2	**1.3**	-1.8	-2.7	$\cdots$
NG15	**1.6**	-0.8	0.05	0.5

interpretation (or a different CGW signal) is preferred, then our work should prove useful in the future to disentangle additional contributions from cosmological sources (see, e.g., [137,138]).

We have shown that a CT spectrum remains compatible with the PTA signal in both IPTA-DR2 and NG15 datasets with a much reduced tension compared to the commonly employed $n_T = 3$ approximation, while it provides a similar fit to NG15 as simple SMBHB models.

The detection of a CT signal would have dramatic implications for particle physics, most likely pointing to the breaking of a (global or gauge) symmetry in a dark sector (DS), for instance, via a PT (or causing the annihilation of domain walls for discrete symmetries) at temperatures $T \gtrsim$ GeV. Some macroscopic properties of the corresponding GW source can be estimated rather model independently. A large GWB amplitude requires a significant energy fraction $\alpha_\star \equiv [\rho_{\text{DS}}/(3H^2 M_p^2)]_{T=T_\star}$ of their source. Either this is the SM (e.g., a first-order PT at QCD confinement which requires additional ingredients [139]), or this energy should decay to SM, because if it remains in dark relativistic species, it contributes as [23]

$$\Delta N_{\text{eff}}^{\text{DS}} \simeq 0.28 \left(\frac{74}{g_*(T_\star)}\right)^{1/3} \left(\frac{\alpha_\star}{0.1}\right). \tag{7}$$

As we detail in [79] (see also [23,25,140]), depending on the model-dependent suppression $\epsilon_\star \lesssim 1$ (e.g., the sub-Hubble size of the source), a cosmological GWB with amplitude $A_{\text{CGW}} \gtrsim 10^{-14.6}$ implies $\alpha_\star \gtrsim 0.07 \epsilon_\star^{-1/2}$ and, therefore, a ΔN_{eff} within the reach of upcoming CMB and LSS surveys [134–136,141]. This conclusion is stronger for a GWB with larger n_t. Alternatively, the required couplings between the SM and the dark sector may be complementarily probed at colliders, laboratory experiments, and astrophysical environments.

Finally, in our work we have conservatively employed the SM prediction for the EOS of the Universe. We notice that the measurement of the CT at PTAs offers a probe of the whole cosmological expansion history up to T_{QCD}, as encapsulated by Eq. (4). Modifications to the CT could occur in BSM scenarios where $w(T)$, $g_*(T)$, or f_{FS} are varied, or if the Universe undergoes a phase of matter domination below the QCD crossover (we present a search for this scenario in [79]). Additionally, PTAs could test the

EOS of hot QCD matter in the early Universe (see, e.g., [139,142]), in the presence of a CT signal.

The near-future detection of a GWB at PTAs could disclose a unique window around the epoch of the QCD crossover. As highlighted in this Letter, this coincidence of scales provides a robust feature to assist in the discrimination between the astrophysical and cosmological origin of the GWB.

---

[*]gabriele.franciolini@uniroma1.it
[†]dracco@stanford.edu
[‡]fabrizio.rompineve@cern.ch

[1] G. Agazie *et al.* (NANOGrav Collaboration), The NANO-Grav 15-year data set: Observations and timing of 68 millisecond pulsars, Astrophys. J. Lett. **951**, L9 (2023).

[2] G. Agazie *et al.* (NANOGrav Collaboration), The NANOGrav 15-year data set: Evidence for a gravitational-wave background, Astrophys. J. Lett. **951**, L8 (2023).

[3] J. Antoniadis *et al.* (EPTA Collaboration), The second data release from the European Pulsar Timing Array I. The dataset and timing analysis, Astron. Astrophys. **678**, A48 (2023).

[4] J. Antoniadis *et al.* (EPTA Collaboration), The second data release from the European Pulsar Timing Array III. Search for gravitational wave signals, Astron. Astrophys. **678**, A50 (2023).

[5] A. Zic *et al.* (PPTA Collaboration), The Parkes Pulsar Timing Array third data release, Pub. Astron. Soc. Aust. **40**, e049 (2023).

[6] D. Reardon *et al.* (PPTA Collaboration), Search for an isotropic gravitational-wave background with the Parkes Pulsar Timing Array, Astrophys. J. Lett. **951**, L6 (2023).

[7] H. Xu *et al.* (CPTA Collaboration), Searching for the nano-Hertz stochastic gravitational wave background with the Chinese Pulsar Timing Array data release I, Res. Astron. Astrophys. **23**, 075024 (2023).

[8] Z. Arzoumanian *et al.* (NANOGrav Collaboration), The NANOGrav 12.5 yr data set: Search for an isotropic stochastic gravitational-wave background, Astrophys. J. Lett. **905**, L34 (2020).

[9] B. Goncharov *et al.*, On the evidence for a common-spectrum process in the search for the nanohertz gravitational-wave background with the Parkes Pulsar Timing Array, Astrophys. J. Lett. **917**, L19 (2021).

[10] S. Chen *et al.*, Common-red-signal analysis with 24-yr high-precision timing of the European Pulsar Timing Array: Inferences in the stochastic gravitational-wave background search, Mon. Not. R. Astron. Soc. **508**, 4970 (2021).

[11] J. Antoniadis *et al.*, The International Pulsar Timing Array second data release: Search for an isotropic gravitational wave background, Mon. Not. R. Astron. Soc. **510**, 4873 (2022).

[12] S. Burke-Spolaor *et al.*, The astrophysics of nanohertz gravitational waves, Astron. Astrophys. Rev. **27**, 5 (2019).

[13] N. S. Pol *et al.* (NANOGrav Collaboration), Astrophysics milestones for Pulsar Timing Array gravitational-wave detection, Astrophys. J. Lett. **911**, L34 (2021).

[14] G. Agazie *et al.* (NANOGrav Collaboration), The NANOGrav 15-year data set: Constraints on supermassive black hole binaries from the gravitational wave background, Astrophys. J. Lett. **952**, L37 (2023).

[15] H. Middleton, A. Sesana, S. Chen, A. Vecchio, W. Del Pozzo, and P. A. Rosado, Massive black hole binary systems and the NANOGrav 12.5 yr results, Mon. Not. R. Astron. Soc. **502**, L99 (2021).

[16] J. Antoniadis *et al.* (EPTA Collaboration), The second data release from the European Pulsar Timing Array: V. implications for massive black holes, dark matter and the early universe, arXiv:2306.16227.

[17] E. Witten, Cosmic separation of phases, Phys. Rev. D **30**, 272 (1984).

[18] A. Vilenkin, Gravitational field of vacuum domain walls and strings, Phys. Rev. D **23**, 852 (1981).

[19] S. Matarrese, S. Mollerach, and M. Bruni, Second order perturbations of the Einstein-de Sitter universe, Phys. Rev. D **58**, 043504 (1998).

[20] L. Bian, R.-G. Cai, J. Liu, X.-Y. Yang, and R. Zhou, Evidence for different gravitational-wave sources in the NANOGrav dataset, Phys. Rev. D **103**, L081301 (2021).

[21] Z. Arzoumanian *et al.* (NANOGrav Collaboration), Searching for gravitational waves from cosmological phase transitions with the NANOGrav 12.5-year dataset, Phys. Rev. Lett. **127**, 251302 (2021).

[22] X. Xue, L. Bian, J. Shu, Q. Yuan, X. Zhu *et al.*, Constraining cosmological phase transitions with the Parkes Pulsar Timing Array, Phys. Rev. Lett. **127**, 251303 (2021).

[23] R. Z. Ferreira, A. Notari, O. Pujolas, and F. Rompineve, Gravitational waves from domain walls in Pulsar Timing Array datasets, J. Cosmol. Astropart. Phys. 02 (2023) 001.

[24] V. Dandoy, V. Domcke, and F. Rompineve, Search for scalar induced gravitational waves in the International Pulsar Timing Array Data Release 2 and NANOgrav 12.5 years dataset, SciPost Phys. Core **6**, 060 (2023).

[25] T. Bringmann, P. F. Depta, T. Konstandin, K. Schmidt-Hoberg, and C. Tasillo, Does NANOGrav observe a dark sector phase transition?, J. Cosmol. Astropart. Phys. 11 (2023) 053.

[26] A. Afzal *et al.* (NANOGrav Collaboration), The NANOGrav 15-year data set: Search for signals from new physics, Astrophys. J. Lett. **951**, L11 (2023).

[27] Z.-C. Chen, C. Yuan, and Q.-G. Huang, Pulsar Timing Array constraints on primordial black holes with NANOGrav 11-year dataset, Phys. Rev. Lett. **124**, 251101 (2020).

[28] Y. Nakai, M. Suzuki, F. Takahashi, and M. Yamada, Gravitational waves and dark radiation from dark phase transition: Connecting NANOGrav Pulsar Timing Data and Hubble Tension, Phys. Lett. B **816**, 136238 (2021).

[29] V. Vaskonen and H. Veermäe, Did NANOGrav see a signal from primordial black hole formation?, Phys. Rev. Lett. **126**, 051303 (2021).

[30] V. De Luca, G. Franciolini, and A. Riotto, NANOGrav data hints at primordial black holes as dark matter, Phys. Rev. Lett. **126**, 041303 (2021).

[31] A. Neronov, A. Roper Pol, C. Caprini, and D. Semikoz, NANOGrav signal from magnetohydrodynamic turbulence at the QCD phase transition in the early Universe, Phys. Rev. D **103**, 041302 (2021).

[32] Z.-C. Zhao and S. Wang, Bayesian implications for the primordial black holes from NANOGrav's Pulsar-Timing Data using the scalar-induced gravitational waves, Universe **9**, 157 (2023).

[33] A. Roper Pol, C. Caprini, A. Neronov, and D. Semikoz, Gravitational wave signal from primordial magnetic fields in the Pulsar Timing Array frequency band, Phys. Rev. D **105**, 123502 (2022).

[34] J. Ellis and M. Lewicki, Cosmic string interpretation of NANOGrav Pulsar Timing Data, Phys. Rev. Lett. **126**, 041304 (2021).

[35] S. Blasi, V. Brdar, and K. Schmitz, Has NANOGrav found first evidence for cosmic strings?, Phys. Rev. Lett. **126**, 041305 (2021).

[36] S. Vagnozzi, Implications of the NANOGrav results for inflation, Mon. Not. R. Astron. Soc. **502**, L11 (2021).

[37] J. J. Blanco-Pillado, K. D. Olum, and J. M. Wachter, Comparison of cosmic string and superstring models to NANOGrav 12.5-year results, Phys. Rev. D **103**, 103512 (2021).

[38] Y. Aoki, G. Endrodi, Z. Fodor, S. D. Katz, and K. K. Szabo, The Order of the quantum chromodynamics transition predicted by the standard model of particle physics, Nature (London) **443**, 675 (2006).

[39] S. Borsanyi *et al.*, Calculation of the axion mass based on high-temperature lattice quantum chromodynamics, Nature (London) **539**, 69 (2016).

[40] D. J. Schwarz, Evolution of gravitational waves through cosmological transitions, Mod. Phys. Lett. A **13**, 2771 (1998).

[41] Y. Watanabe and E. Komatsu, Improved calculation of the primordial gravitational wave spectrum in the standard model, Phys. Rev. D **73**, 123515 (2006).

[42] S. Schettler, T. Boeckel, and J. Schaffner-Bielich, Imprints of the QCD phase transition on the spectrum of gravitational waves, Phys. Rev. D **83**, 064030 (2011).

[43] A. Hook, G. Marques-Tavares, and D. Racco, Causal gravitational waves as a probe of free streaming particles and the expansion of the Universe, J. High Energy Phys. 02 (2021) 117.

[44] D. Brzeminski, A. Hook, and G. Marques-Tavares, Precision early universe cosmology from stochastic gravitational waves, J. High Energy Phys. 11 (2022) 061.

[45] M. Loverde and Z. J. Weiner, Probing neutrino interactions and dark radiation with gravitational waves, J. Cosmol. Astropart. Phys. 02 (2023) 064.

[46] B. B. P. Perera *et al.*, The International Pulsar Timing Array: Second data release, Mon. Not. R. Astron. Soc. **490**, 4666 (2019).

[47] N. Seto and J. Yokoyama, Probing the equation of state of the early universe with a space laser interferometer, J. Phys. Soc. Jpn. **72**, 3082 (2003).

[48] S. Weinberg, Damping of tensor modes in cosmology, Phys. Rev. D **69**, 023503 (2004).

[49] L. A. Boyle and P. J. Steinhardt, Probing the early universe with inflationary gravitational waves, Phys. Rev. D **77**, 063504 (2008).

[50] L. A. Boyle and A. Buonanno, Relating gravitational wave constraints from primordial nucleosynthesis, pulsar timing, laser interferometers, and the CMB: Implications for the early Universe, Phys. Rev. D **78**, 043531 (2008).

[51] C. Caprini, R. Durrer, T. Konstandin, and G. Servant, General properties of the gravitational wave spectrum from phase transitions, Phys. Rev. D **79**, 083519 (2009).

[52] R. Jinno, T. Moroi, and K. Nakayama, Probing dark radiation with inflationary gravitational waves, Phys. Rev. D **86**, 123502 (2012).

[53] C. Caprini *et al.*, Science with the space-based interferometer eLISA. II: Gravitational waves from cosmological phase transitions, J. Cosmol. Astropart. Phys. 04 (2016) 001.

[54] G. Barenboim and W.-I. Park, Gravitational waves from first order phase transitions as a probe of an early matter domination era and its inverse problem, Phys. Lett. B **759**, 430 (2016).

[55] M. Geller, A. Hook, R. Sundrum, and Y. Tsai, Primordial anisotropies in the gravitational wave background from cosmological phase transitions, Phys. Rev. Lett. **121**, 201303 (2018).

[56] K. Saikawa and S. Shirai, Primordial gravitational waves, precisely: The role of thermodynamics in the Standard Model, J. Cosmol. Astropart. Phys. 05 (2018) 035.

[57] Y. Cui, M. Lewicki, D. E. Morrissey, and J. D. Wells, Probing the pre-BBN universe with gravitational waves from cosmic strings, J. High Energy Phys. 01 (2019) 081.

[58] R. R. Caldwell, T. L. Smith, and D. G. E. Walker, Using a primordial gravitational wave background to illuminate new physics, Phys. Rev. D **100**, 043513 (2019).

[59] C. Caprini and D. G. Figueroa, Cosmological backgrounds of gravitational waves, Classical Quantum Gravity **35**, 163001 (2018).

[60] R.-G. Cai, S. Pi, and M. Sasaki, Universal infrared scaling of gravitational wave background spectra, Phys. Rev. D **102**, 083528 (2020).

[61] F. D'Eramo and K. Schmitz, Imprint of a scalar era on the primordial spectrum of gravitational waves, Phys. Rev. Res. **1**, 013010 (2019).

[62] N. Bernal and F. Hajkarim, Primordial gravitational waves in nonstandard cosmologies, Phys. Rev. D **100**, 063502 (2019).

[63] D. G. Figueroa and E. H. Tanin, Ability of LIGO and LISA to probe the equation of state of the early Universe, J. Cosmol. Astropart. Phys. 08 (2019) 011.

[64] P. Auclair *et al.*, Probing the gravitational wave background from cosmic strings with LISA, J. Cosmol. Astropart. Phys. 04 (2020) 034.

[65] C.-F. Chang and Y. Cui, Stochastic gravitational wave background from global cosmic strings, Phys. Dark Universe **29**, 100604 (2020).

[66] F. Hajkarim and J. Schaffner-Bielich, Thermal history of the early universe and primordial gravitational waves from induced scalar perturbations, Phys. Rev. D **101**, 043522 (2020).

[67] C. Caprini *et al.*, Detecting gravitational waves from cosmological phase transitions with LISA: An update, J. Cosmol. Astropart. Phys. 03 (2020) 024.

[68] Y. Gouttenoire, G. Servant, and P. Simakachorn, Beyond the standard models with cosmic strings, J. Cosmol. Astropart. Phys. 07 (2020) 032.

[69] Y. Gouttenoire, G. Servant, and P. Simakachorn, BSM with cosmic strings: Heavy, up to EeV mass, unstable particles, J. Cosmol. Astropart. Phys. 07 (2020) 016.

[70] G. Domènech, Induced gravitational waves in a general cosmological background, Int. J. Mod. Phys. D **29**, 2050028 (2020).

[71] H.-K. Guo, K. Sinha, D. Vagie, and G. White, Phase transitions in an expanding universe: Stochastic gravitational waves in standard and non-standard histories, J. Cosmol. Astropart. Phys. 01 (2021) 001.

[72] J. Ellis, M. Lewicki, and V. Vaskonen, Updated predictions for gravitational waves produced in a strongly supercooled phase transition, J. Cosmol. Astropart. Phys. 11 (2020) 020.

[73] S. Blasi, V. Brdar, and K. Schmitz, Fingerprint of low-scale leptogenesis in the primordial gravitational-wave spectrum, Phys. Rev. Res. **2**, 043321 (2020).

[74] G. Domènech, S. Pi, and M. Sasaki, Induced gravitational waves as a probe of thermal history of the universe, J. Cosmol. Astropart. Phys. 08 (2020) 017.

[75] R. Allahverdi *et al.*, The first three seconds: A review of possible expansion histories of the early universe, Open J. Astrophys. **4**, 1 (2021).

[76] J. Berger, A. Bhoonah, and B. Padhi, Probing exotic phases via stochastic gravitational wave spectra, arXiv:2306.07283.

[77] M. B. Hindmarsh, M. Lüben, J. Lumma, and M. Pauly, Phase transitions in the early universe, SciPost Phys. Lect. Notes **24**, 1 (2021).

[78] P. Athron, C. Balázs, A. Fowlie, L. Morris, and L. Wu, Cosmological phase transitions: From perturbative particle physics to gravitational waves, Prog. Part. Nucl. Phys. **135**, 104094 (2024).

[79] See Supplemental Material at http://link.aps.org/supplemental/10.1103/PhysRevLett.132.081001 for details on the relation between frequency today and temperature at horizon crossing, the tabulated causality tail signal, implications for particle physics, effects of intermediate matter domination, and our numerical strategy, which includes Refs. [2,11,20,21,23,24,29,30,43,59,66,70,80–122].

[80] J. A. Ellis, M. Vallisneri, S. R. Taylor, and P. T. Baker, ENTERPRISE: Enhanced Numerical Toolbox Enabling a Robust PulsaR Inference SuitE (v3.0.0), 10.5281/zenodo.4059815.

[81] S. R. Taylor, P. T. Baker, J. S. Hazboun, J. Simon, and S. J. Vigeland, enterprise_extensions (2021), v2.3.3.

[82] J. Ellis and R. van Haasteren, jellis18/PTMCMCSampler: Official Release (1.0.0), 10.5281/zenodo.1037579.

[83] A. Mitridate, D. Wright, R. von Eckardstein, T. Schröder, J. Nay, K. Olum, K. Schmitz, and T. Trickle, PTArcade, arXiv:2306.16377.

[84] C. Patrignani *et al.* (Particle Data Group Collaboration), Review of particle physics, Chin. Phys. C **40**, 100001 (2016).

[85] E. W. Kolb and M. S. Turner, *The Early Universe* (CRC Press, Boca Raton, 1990), Vol. 69.

[86] R. w. Hellings and G. s. Downs, Upper limits on the isotropic gravitational radiation background from pulsar timing analysis, Astrophys. J. Lett. **265**, L39 (1983).

[87] S. Borsányi, Z. Fodor, J. N. Guenther, R. Kara, S. D. Katz, P. Parotto, A. Pásztor, C. Ratti, and K. K. Szabó, Lattice QCD equation of state at finite chemical potential from an alternative expansion scheme, Phys. Rev. Lett. **126**, 232001 (2021).

[88] J. S. Hazboun, J. D. Romano, and T. L. Smith, Realistic sensitivity curves for Pulsar Timing Arrays, Phys. Rev. D **100**, 104028 (2019).

[89] W. DeRocco and J. A. Dror, Using pulsar parameter drifts to detect sub-nanohertz gravitational waves (2022).

[90] W. DeRocco and J. A. Dror, Searching For stochastic gravitational waves below a nanohertz, Phys. Rev. D **108**, 103011 (2023).

[91] P. Jiang *et al.*, Commissioning progress of the FAST, Sci. China Phys. Mech. Astron. **62**, 959502 (2019).

[92] M. T. Miles *et al.*, The MeerKAT Pulsar Timing Array: First data release, Mon. Not. R. Astron. Soc. **519**, 3976 (2023).

[93] D. E. Kaplan, M. A. Luty, and K. M. Zurek, Asymmetric dark matter, Phys. Rev. D **79**, 115016 (2009).

[94] R. Foot and R. R. Volkas, Was ordinary matter synthesized from mirror matter? An attempt to explain why Omega (Baryon) approximately equal to 0.2 Omega(Dark), Phys. Rev. D **68**, 021304(R) (2003).

[95] R. Foot and R. R. Volkas, Explaining Omega(Baryon) approximately 0.2 Omega(Dark) through the synthesis of ordinary matter from mirror matter: A more general analysis, Phys. Rev. D **69**, 123510 (2004).

[96] S. J. Lonsdale and R. R. Volkas, Grand unified hidden-sector dark matter, Phys. Rev. D **90**, 083501 (2014); **91**, 129906(E) (2015).

[97] S. J. Lonsdale, Unified dark matter with intermediate symmetry breaking scales, Phys. Rev. D **91**, 125019 (2015).

[98] S. J. Lonsdale and R. R. Volkas, Comprehensive asymmetric dark matter model, Phys. Rev. D **97**, 103510 (2018).

[99] C. Murgui and K. M. Zurek, Dark unification: A UV-complete theory of asymmetric dark matter, Phys. Rev. D **105**, 095002 (2022).

[100] P. Baratella, A. Pomarol, and F. Rompineve, The supercooled universe, J. High Energy Phys. 03 (2019) 100.

[101] W. DeRocco, P. W. Graham, D. Kasen, G. Marques-Tavares, and S. Rajendran, Supernova signals of light dark matter, Phys. Rev. D **100**, 075018 (2019).

[102] V. Acquaviva, N. Bartolo, S. Matarrese, and A. Riotto, Second order cosmological perturbations from inflation, Nucl. Phys. **B667**, 119 (2003).

[103] S. Mollerach, D. Harari, and S. Matarrese, CMB polarization from secondary vector and tensor modes, Phys. Rev. D **69**, 063002 (2004).

[104] D. Baumann, P. J. Steinhardt, K. Takahashi, and K. Ichiki, Gravitational wave spectrum induced by primordial scalar perturbations, Phys. Rev. D **76**, 084019 (2007).

[105] J. R. Espinosa, D. Racco, and A. Riotto, A cosmological signature of the SM Higgs instability: Gravitational waves, J. Cosmol. Astropart. Phys. 09 (2018) 012.

[106] K. Kohri and T. Terada, Semianalytic calculation of gravitational wave spectrum nonlinearly induced from primordial curvature perturbations, Phys. Rev. D **97**, 123532 (2018).

[107] R. Saito and J. Yokoyama, Gravitational wave background as a probe of the primordial black hole abundance, Phys. Rev. Lett. **102**, 161101 (2009); **107**, 069901(E) (2011).

[108] K. Kohri and T. Terada, Solar-mass primordial black holes explain NANOGrav hint of gravitational waves, Phys. Lett. B **813**, 136040 (2021).

[109] S. Sugiyama, V. Takhistov, E. Vitagliano, A. Kusenko, M. Sasaki, and M. Takada, Testing stochastic gravitational wave signals from primordial black holes with optical telescopes, Phys. Lett. B **814**, 136097 (2021).

[110] G. Domènech and S. Pi, NANOGrav hints on planet-mass primordial black holes, Sci. China Phys. Mech. Astron. **65**, 230411 (2022).

[111] K. Inomata, M. Kawasaki, K. Mukaida, and T. T. Yanagida, NANOGrav results and LIGO-Virgo primordial

black holes in axionlike curvaton models, Phys. Rev. Lett. **126**, 131301 (2021).

[112] G. Franciolini and A. Urbano, Primordial black hole dark matter from inflation: The reverse engineering approach, Phys. Rev. D **106**, 123519 (2022).

[113] G. Franciolini, I. Musco, P. Pani, and A. Urbano, From inflation to black hole mergers and back again: Gravitational-wave data-driven constraints on inflationary scenarios with a first-principle model of primordial black holes across the QCD epoch, Phys. Rev. D **106**, 123526 (2022).

[114] G. Ferrante, G. Franciolini, A. Iovino, Jr., and A. Urbano, Primordial black holes in the curvaton model: Possible connections to pulsar timing arrays and dark matter, J. Cosmol. Astropart. Phys. 06 (2023) 057.

[115] M. Sasaki, T. Suyama, T. Tanaka, and S. Yokoyama, Primordial black holes—perspectives in gravitational wave astronomy, Classical Quantum Gravity **35**, 063001 (2018).

[116] B. Carr, K. Kohri, Y. Sendouda, and J. Yokoyama, Constraints on primordial black holes, Rep. Prog. Phys. **84**, 116902 (2021).

[117] G. Franciolini, A. Iovino, Junior., V. Vaskonen, and H. Veermae, The recent gravitational wave observation by pulsar timing arrays and primordial black holes: The importance of non-Gaussianities, Phys. Rev. Lett. **131**, 201401 (2023).

[118] K. T. Abe, Y. Tada, and I. Ueda, Induced gravitational waves as a cosmological probe of the sound speed during the QCD phase transition, J. Cosmol. Astropart. Phys. 06 (2021) 048.

[119] M. Gorghetto, E. Hardy, and H. Nicolaescu, Observing invisible axions with gravitational waves, J. Cosmol. Astropart. Phys. 06 (2021) 034.

[120] R. Jinno and M. Takimoto, Gravitational waves from bubble collisions: An analytic derivation, Phys. Rev. D **95**, 024009 (2017).

[121] M. Hindmarsh, S. J. Huber, K. Rummukainen, and D. J. Weir, Shape of the acoustic gravitational wave power spectrum from a first order phase transition, Phys. Rev. D **96**, 103520 (2017); **101**, 089902(E) (2020).

[122] A. Lewis, GetDist: A PYTHON package for analysing Monte Carlo samples, arXiv:1910.13970.

[123] Z. Haiman, Z. Haiman, B. Kocsis, B. Kocsis, K. Menou, and K. Menou, The population of viscosity- and gravitational wave-driven supermassive black hole binaries among luminous AGN, Astrophys. J. **700**, 1952 (2009); **937**, 129(E) (2022).

[124] B. Kocsis and A. Sesana, Gas driven massive black hole binaries: Signatures in the nHz gravitational wave background, Mon. Not. R. Astron. Soc. **411**, 1467 (2011).

[125] Z. Pan, Z. Lyu, and H. Yang, Wet extreme mass ratio inspirals may be more common for spaceborne gravitational wave detection, Phys. Rev. D **104**, 063007 (2021).

[126] J. Ellis, M. Fairbairn, G. Hütsi, M. Raidal, J. Urrutia, V. Vaskonen, and H. Veermäe, Prospects for future binary

black hole GW studies in light of PTA measurements, Astron. Astrophys. **676**, A38 (2023).

[127] M. M. Kozhikkal, S. Chen, G. Theureau, M. Habouzit, and A. Sesana, Mass-redshift dependency of supermassive black hole binaries for the gravitational wave background, arXiv:2305.18293.

[128] E. S. Phinney, A Practical theorem on gravitational wave backgrounds, arXiv:astro-ph/0108028.

[129] N. Aghanim et al. (Planck Collaboration), Planck 2018 results. VI. Cosmological parameters, Astron. Astrophys. **641**, A6 (2020); **652**, C4(E) (2021).

[130] D. Cutting, E. G. Escartin, M. Hindmarsh, and D. J. Weir, Gravitational waves from vacuum first order phase transitions II: From thin to thick walls, Phys. Rev. D **103**, 023531 (2021).

[131] R. Jinno, T. Konstandin, and H. Rubira, A hybrid simulation of gravitational wave production in first-order phase transitions, J. Cosmol. Astropart. Phys. 04 (2021) 014.

[132] C. J. Moore and A. Vecchio, Ultra-low-frequency gravitational waves from cosmological and astrophysical processes, Nat. Astron. **5**, 1268 (2021).

[133] G. Agazie et al. (International Pulsar Timing Array Collaboration), Comparing recent PTA results on the nanohertz stochastic gravitational wave background, arXiv:2309.00693.

[134] K. Abazajian et al. (CMB-S4 Collaboration), Snowmass 2021 CMB-S4 White Paper, arXiv:2203.08024.

[135] A. Aghamousa et al. (DESI Collaboration), The DESI experiment part I: Science, targeting, and survey design, arXiv:1611.00036.

[136] L. Amendola et al., Cosmology and fundamental physics with the Euclid satellite, Living Rev. Relativity **21**, 2 (2018).

[137] A. R. Kaiser, N. S. Pol, M. A. McLaughlin, S. Chen, J. S. Hazboun, L. Z. Kelley, J. Simon, S. R. Taylor, S. J. Vigeland, and C. A. Witt, Disentangling multiple stochastic gravitational wave background sources in PTA data sets, Astrophys. J. **938**, 115 (2022).

[138] G. Sato-Polito and M. Kamionkowski, Exploring the spectrum of stochastic gravitational-wave anisotropies with Pulsar Timing Arrays, arXiv:2305.05690.

[139] D. Bödeker, F. Kühnel, I. M. Oldengott, and D. J. Schwarz, Lepton flavor asymmetries and the mass spectrum of primordial black holes, Phys. Rev. D **103**, 063506 (2021).

[140] Y. Bai and M. Korwar, Cosmological constraints on first-order phase transitions, Phys. Rev. D **105**, 095015 (2022).

[141] P. Ade et al. (Simons Observatory Collaboration), The Simons Observatory: Science goals and forecasts, J. Cosmol. Astropart. Phys. 02 (2019) 056.

[142] P. Achenbach et al., The present and future of QCD, arXiv:2303.02579.

[143] W. G. Lamb, S. R. Taylor, and R. van Haasteren, The need for speed: Rapid refitting techniques for Bayesian spectral characterization of the gravitational wave background using PTAs, Phys. Rev. D **108**, 103019 (2023).